Published in Journal of Applied Physics 77, issue 2, 712-716, 1995
which should be used for any reference to this work

Electrical properties and degradation kinetics of compensated hydrogenated microcrystalline silicon deposited by very high-frequency-glow discharge

R. Flückiger, J. Meier, M. Goetz, and A. Shah
Institut de Microtechnique, Université de Neuchâtel, rue Breguet 2, 2000 Neuchâtel, Switzerland

Microcrystalline silicon (μc-Si:H) layers deposited by the very high-frequency-glow discharge technique at a radio-frequency excitation of 70 MHz are observed to be basically slightly ⟨n⟩ type. By doping (so-called "microdoping") with boron in the gas phase volume part per million (vppm) range, compensated material could be obtained. The influence of this doping on the electronic transport properties is documented. A pronounced onset of the boron incorporation into the films measured by secondary-ion-mass spectrometry is observed around 3 vppm (B_2H_6/SiH_4), together with marked changes in the electrical properties. The compensated film obtained for a microdoping of about 1 vppm shows the lowest dark conductivity $[3\times10^{-8}\ (\Omega\ \mathrm{cm})^{-1}]$, the highest activation energy (517 meV), and, finally, the highest photoconductive gain of 6×10^3 (photo/dark current ratio). Depending on the value of the activation energy (the critical value is ≈0.2 eV), two different transport models are identified, corresponding to "Meyer–Neldel" or "anti-Meyer–Neldel" behavior. As for light-induced degradation, the compensated film exhibits better stability than undoped films. Finally, the use of slightly boron doped μc-Si:H as photovoltaically active material will be discussed.

I. INTRODUCTION

Since the discovery in 1977 of the "Staebler–Wronski effect"[1] in hydrogenated amorphous silicon material (a-Si:H), a wide effort is being undertaken to obtain more stable material, especially for photovoltaic applications. Until now, this problem has not been fully solved. Preliminary work done with hydrogenated microcrystalline silicon (μc-Si:H)[2–4] shows that this material does not degrade as much as a-Si:H and that it has the potential to become a new material for photovoltaic devices.[5] Our group has therefore investigated here μc-Si:H in more detail.

Our earlier studies have shown[6–8] that the very high-frequency-glow discharge (VHFGD) technique at 70 MHz is especially favorable for the growth of μc-Si:H. In fact, both the input power and the deposition temperature can be kept lower than in the case of conventional 13.56 MHz GD, as was shown in our previous work.[9] Based on plasma diagnostics with VHF plasmas,[10] we postulate that two effects are involved: first, lower ion bombardment energies than at 13.56 MHz—these being due to a reduced sheath potential and second, a higher atomic hydrogen flux on the growth surface; we suggest that both effects contribute to favorable growth conditions for μc-Si:H.

Microcrystalline silicon has, in general, lower optical absorption in the visible than amorphous silicon. It has, however, higher absorption in the infrared range.[5] Because of these properties, fully microcrystalline *p-i-n* diodes may find their use within tandem structures, and it is towards this goal that we have studied intrinsic μc-Si:H layers.

As previously reported,[9] we found that undoped μc-Si:H has a slightly ⟨n⟩-type character, this being already reported in earlier work.[3,11] Now, in the present study, we will try to obtain more insight into the doping compensation mechanism of μc-Si:H. Compensated layers are deposited by adding low quantities of diborane into the plasma gas. The stability of such compensated μc-Si:H films was analyzed under strong light illumination (fast degradation) and a detailed study of the electrical transport properties as a function of the doping level has been undertaken. The interpretation of our results is based on previous transport studies on microcrystalline silicon.[12–15]

II. EXPERIMENT

All films reported on were deposited in a single chamber reactor by the capacitively coupled glow discharge method at a plasma excitation frequency of 70 MHz (VHFGD).[16,17] In order to compensate the μc-Si:H material in the vppm doping range (a technique we will henceforth call "microdoping"), an additional mixing chamber was installed at the process chamber. To avoid cross contamination from the outgassing, the chamber walls were heated overnight and kept at room temperature for the deposition.

The gases used were silane (SiH_4), hydrogen (H_2), and diborane (B_2H_6). The films were deposited onto Dow Corning 7059 glass and on polished single-crystal silicon wafers with ⟨100⟩ orientation, at dilution level of 3% silane in hydrogen and a total gas flow of about 100 SCCM. The microdoping ratio (B_2H_6/SiH_4) was varied between 0 (undoped) and 10 vppm. The power measured was 3 W; this corresponds to a very low power density of only 23 mW/cm^2 in the plasma, even if one neglects the matching losses. The substrate deposition temperature T_{dep} was 220 °C and the gas pressure was kept at 0.4 mbar.

The film thicknesses—measured with a step profiler on a step etched out with a KOH solution—were in the range of 0.4 μm. The deposition rates obtained were around 0.5 Å/s. The conductivity [dark conductivity σ_d and photoconductivity σ_{photo} (at 100 mW/cm^2)] and the dark conductivity acti-

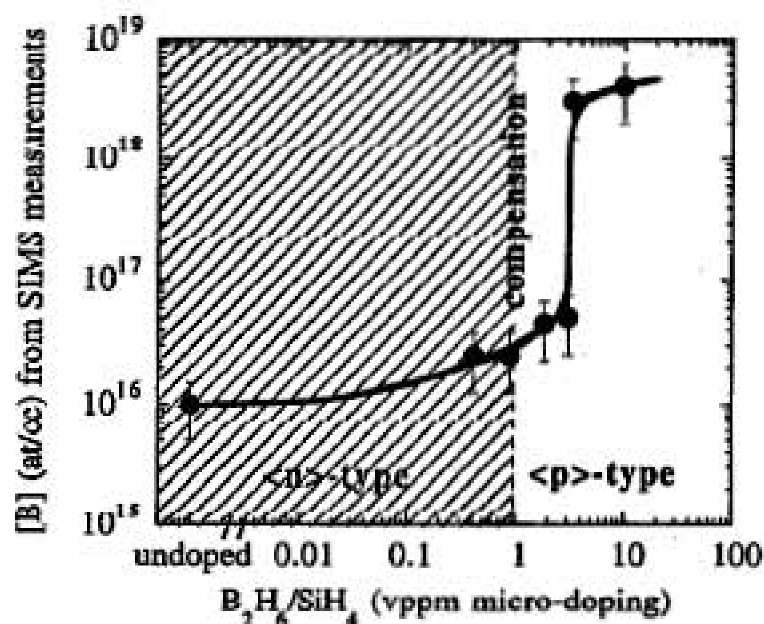

FIG. 1. Boron concentration [B] (at/cc) in the films (bulk values) measured by SIMS as a function of the microdoping ratio (B_2H_6/SiH_4) in volume part per million. The undoped film is arbitrarily placed at the left-hand side of the x axis.

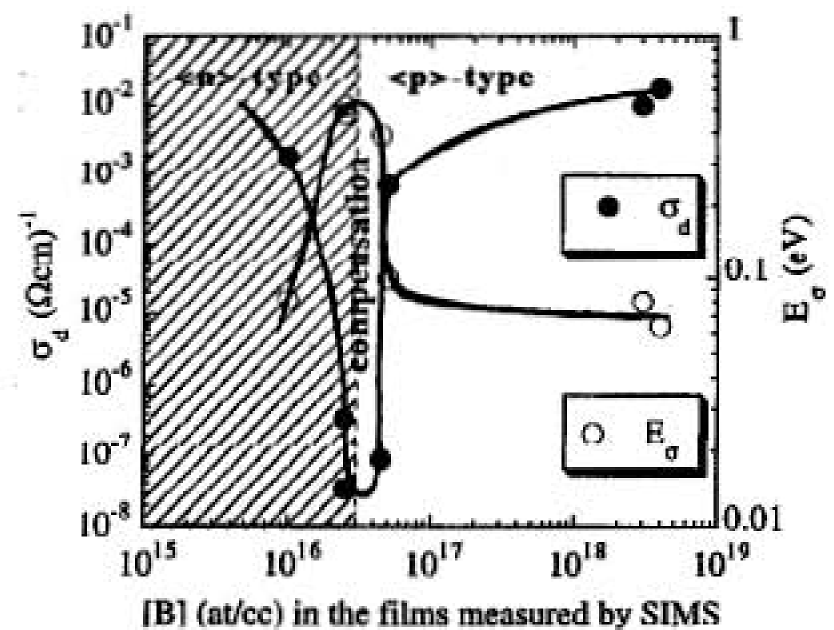

FIG. 2. Dark conductivity σ_d (at room temperature) and activation energy E_σ as a function of the boron concentration [B] (at/cc) measured in the film (bulk values) by SIMS. The compensation point is obtained at a doping of about 1 vppm (B_2H_6/SiH_4) corresponding to a boron concentration of about 3×10^{16} (at/cc) in the film.

vation energy E_σ were all measured using two coplanar aluminum contacts (1000 Å thick) under vacuum conditions ($\sim10^{-6}$ mbar), after a standard annealing step. The activation energy values were extracted from the plot of the conductivity in the lower range of temperature [room temperature (RT) up to about 100 °C]. The films were further analyzed by infrared (IR) and ultraviolet visible transmission spectroscopy. The subgap absorption was determined from PDS (photothermal deflection spectroscopy) and calibrated with an optical transmission measurement in the visible range. SIMS (secondary-ion-mass spectroscopy) measurements were carried out to determine the doping concentrations (B and P) and, further, the concentrations of contaminants (H, C, N, O) of the films. The photoconductivity of three typical films was analyzed under long-term illumination with an intensive high-pressure sodium lamp (1.5×10^{18} photons/cm^2 s). With the absorption coefficient of about 1×10^4 cm^{-1} for our μc-Si:H material and with the wavelength of this light source of 590 nm, we obtain a relatively uniform illumination throughout the entire film (transmission $\sim$70%). The temperature during the light exposure was 40° C and was measured by an IR thermometer. Structural characterization techniques (transmission electron microscopy, x ray, Raman) prove the high crystalline volume fraction of the material (around 80%–90%); these results are, however, not shown in this paper.

III. RESULTS AND DISCUSSION

To judge the results of the degradation studies we have first to understand the effects of the compensation experiments. The slightly $\langle n\rangle$-type character of the "undoped" as-grown μc-Si:H material (to be termed more precisely as "not intentionally doped") is compensated by systematically adding small amounts of diborane (microdoping) into the gas phase, pushing thus the Fermi level (E_F) towards midgap. Figure 1 shows the boron concentration [B] (at/cc) in the films (bulk values) as a function of the microdoping ratio (B_2H_6/SiH_4) obtained from SIMS measurements. One can observe the pronounced onset of the boron incorporation into the films at a doping value of about 3 vppm. The concentrations of phosphorus, hydrogen, and of major impurities incorporated into the films are constant over all samples and are as follows: $C_P=3\times10^{16}$, $C_H=3\times10^{21}$, $C_O=2\times10^{19}$, $C_C=1.5\times10^{18}$, and $C_N=1\times10^{16}$ (at/cc). As we will see later, the compensated film (lowest dark conductivity and highest activation energy) has a boron concentration of about 3×10^{16} (at/cc) for a microdoping value of about 1 vppm, this value corresponding to the phosphorus concentration mentioned above. So, besides the O and N contaminations, the phosphorous atoms present could possibly also contribute to the slightly $\langle n\rangle$-type character of the undoped films. Other groups[4] have proposed as an alternate explanation that the $\langle n\rangle$ type character is due to the distortion of the network at the transition between crystallites and the surrounding amorphous matrix, leading thereby to a density-of-states distribution that pins E_F at the grain boundaries near the conduction band of the crystallites. Whereas such an effect may also be present, we suggest here that the involuntary incorporation of contaminants and dopants is the main reason behind the $\langle n\rangle$-type character of undoped or, rather, not intentionally doped films.

Figure 2 shows the effect of the compensation experiment on the dark conductivity and on the dark conductivity activation energy as a function of boron concentration [B] (at/cc) measured in the films by SIMS. It can clearly be seen that the Fermi-level position reacts sensitively to the diborane partial pressure via boron incorporation. Microdoping shifts the dark conductivity over a wide range from 2×10^{-3} for the undoped material to 3×10^{-8} (Ω cm)$^{-1}$ at $\sim3\times10^{16}$ B/cc. In the same way, the activation energy increases from 80 to the maximum value of 517 meV. Further doping leads to a very sharp increase of σ_d and to $\langle p\rangle$-type

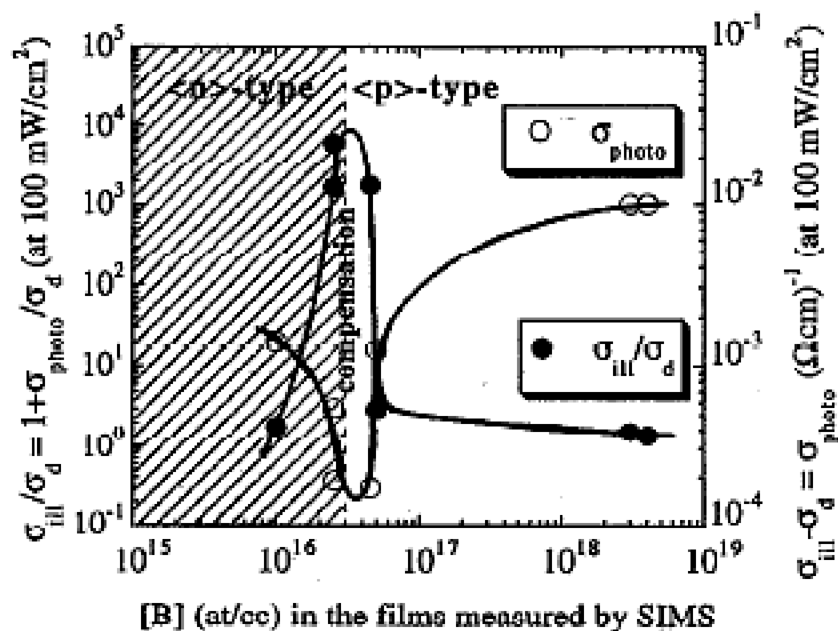

FIG. 3. σ_{ill}/σ_d and σ_{photo} (at 100 mW/cm^2) as a function of the boron concentration [B] (at/cc) in the films measured by SIMS. σ_{ill} is the measured value of conductivity under illumination, σ_d the dark conductivity, and σ_{photo} the calculated photoconductivity (equal to $\sigma_{ill}-\sigma_d$).

material,[3,11,18,19] with values for E_σ that become once again smaller. In analogy with a study of boron doping in polycrystalline silicon,[19] such a sharp increase in the dark conductivity may be interpreted as being the result of the increase in carrier concentration and mobility. [Note that another recent study of our group[20] dealing with compensation by the two types of dopants (P and B) did not lead to such a low dark conductivity value as the one obtained here in the present work.] The plot of the dark conductivity shows for higher temperatures (100–200 °C) a steeper decrease than for temperatures below 100 °C. We plotted the lower values of E_σ which correspond to the RT conductivity points drawn in Fig. 2. The doping ratios needed here to achieve the compensation of the material at ~1 vppm—corresponding to a boron concentration value of about 3×10^{16} at/cc—are significantly lower than those reported in Refs. 3 and 11 using a remote plasma-enhanced chemical-vapor deposition (RPECVD) system; in the latter work, compensation was obtained for a boron concentration of 5×10^{17} (at/cc). Furthermore, the remote PECVD deposition leads to maximum values of E_σ around 0.7 eV,[3,11] i.e., significantly higher than what is found here (0.517 eV). This difference may be due to a higher band gap prevailing in the RPECVD material; possibly, the higher band gap arises from a lower crystalline volume fraction.

In Fig. 3 we plot σ_{ill}/σ_d and σ_{photo} (at 100 mW/cm^2) as a function of the boron concentration (at/cc) in the films as measured by SIMS. To avoid confusion with the notation, we will write

$$\sigma_{ill}=\sigma_{photo}+\sigma_d, \tag{1}$$

with σ_{ill}=conductivity as measured under illumination, σ_{photo}=photoconductivity [calculated from Eq. (1)], and finally σ_d=dark conductivity. σ_{ill}/σ_d shows a curve similar to the one for E_σ; the same is true for σ_{photo} and σ_d. σ_{ill}/σ_d shows a maximum value of about 6×10^3 around compensation, whereas σ_{photo} exhibits a minimum of 1.5×10^{-4} $(\Omega\ \text{cm})^{-1}$. This maximum of the photoconductive gain at 100 mW/cm^2 for our compensated μc-Si:H is a little higher than the one observed in Refs. 3 and 11 and measured there under 0.5 AM1 illumination.These high values of photoconductive gain are an indication that μc-Si:H can indeed be used as a photovoltaically active material. In order to explain the minimum in photoconductivity obtained for compensated μc-Si:H, we propose two possible lines of thought. First, one may compare this minimum to a similar minimum observed in a previous study[21] for compensated amorphous silicon films. It was found there that a transition from one type of dominant free carrier to the other ($n_f \approx p_f$) is responsible for the minimum in photoconductivity observed on this particular compensated film. A similar effect may also prevail in the present series of μc-Si:H films. A second, possible explanation starts from the following general equation for photoconductivity:

$$\sigma_{photo}=e(\mu_p p_f+\mu_n n_f), \tag{2}$$

with $\mu_{p(n)}$=effective mobility of the holes (electrons), $p_f(n_f)$=free-carrier density of the holes (respectively, electrons), and e=elementary charge. By microdoping in the vppm range around the compensation point, we are able to move the Fermi level slightly and this probably did not change very much, neither the material structure, nor the defect density. A direct consequence of this is a corresponding variation in the carrier densities through a variation of the donor or acceptor densities. Now, let us recall the grain-boundary trapping model for μc-Si:H,[12] where the barrier potential between crystallites is a function of the carrier density. Thus if for our compensated film the carrier density is such that the barrier potential has here a maximum value, then automatically the effective mobility and finally the photoconductivity will present here a minimum. Unfortunately, at present we do not have enough transport measurements on these compensated films to be able to discriminate between these two possible explanations.

The absorption in the subgap region as measured by PDS is shown for the compensated film (0.9 vppm) in Fig. 4. The PDS spectra were calibrated at 600 nm from transmission and reflection measurements. The low photon energy (<1 eV) absorption value for this film is <10 cm^{-1} and this is remarkably low for μc-Si:H material. For comparison, a μc-Si:H film compensated by the use of two types of dopants, i.e., P and B (our previous series), shows a value higher than 30 cm^{-1},[20] whereas the high photon energy (>1.5 eV) absorption is very similar for both series. We also measured (but did not plot) the absorption as a function of microdoping in the region 0–3 vppm and observed identical spectra with small variations in the low photon energy absorption values: These variations are less than a factor of 2. Similarly, work done previously on compensated a-Si:H films by our own group[22] showed also roughly constant deep defect densities (constant subgap absorption) as a function of the doping level (in the same range of low-level doping as studied here). The subgap absorption has been related in μc-Si:H material both to deep defects and to free-carrier absorption;[20] we conclude, here, from the low values of subgap absorption observed on our set of films that these are not doped strongly

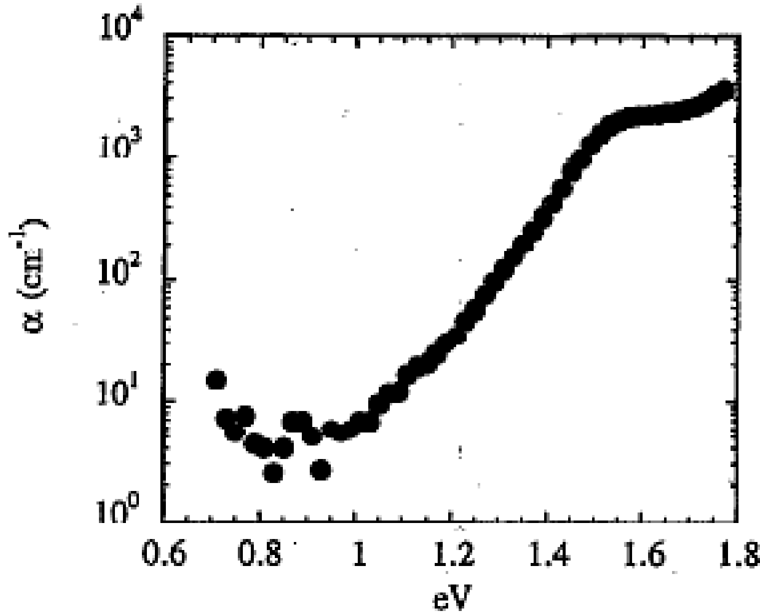

FIG. 4. Absorption of the compensated film (0.9 vppm microdoping) measured by PDS and transmission/reflection data. The calibration of the PDS curve was done at 600 nm (2.07 eV).

enough to observe the effect of the free carriers. Furthermore, it has been concluded from IR transmission spectroscopy measurements on doped μc-Si:H material[20] that the observed base-line shift is related to free-carrier absorption. IR measurements on our compensated series indeed do not show a base-line shift, confirming thus that there is no observable free-carrier absorption.

In order to explain the temperature behavior of the dark conductivity (for the temperature range from RT up to about 100° C) we will now use the usual simple expression for a thermally activated conductivity:

$$\sigma=\sigma_0 \exp(-E_\sigma/KT), \quad (3)$$

with σ_0=conductivity prefactor and E_σ=effective activation energy. This is based on the work of Ref. 14 for VHFGD samples with E_F near midgap. Then, in Fig. 5 we can plot

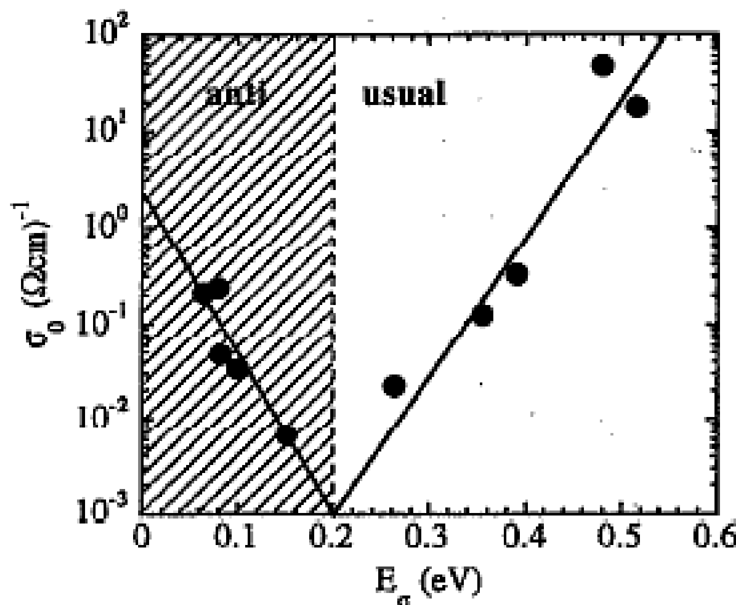

FIG. 5. Dark conductivity data: conductivity prefactor σ_0 as a function of the effective activation energy E_σ.

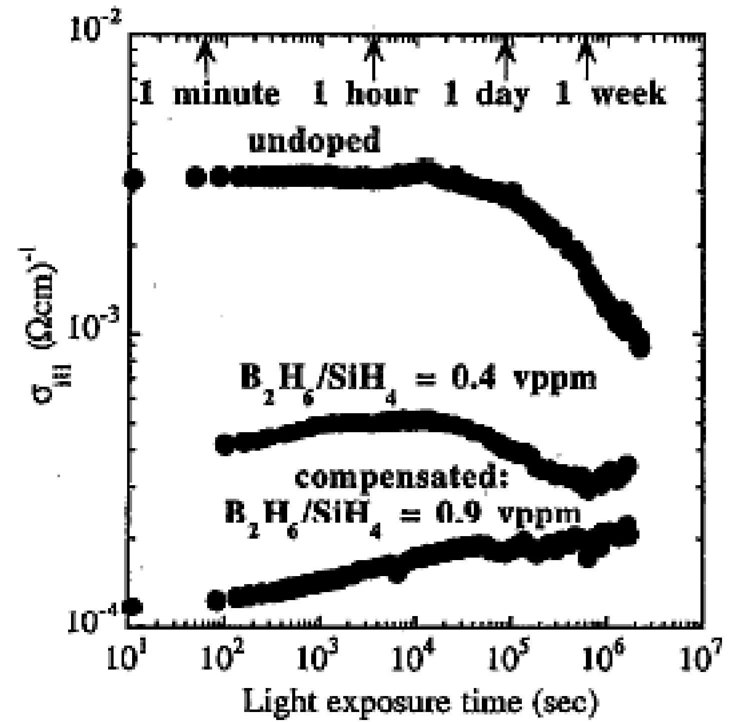

FIG. 6. σ_{ill} for three different samples [undoped, 0.4 vppm, 0.9 vppm (compensated)] from the compensated series as a function of the light exposure time (sodium lamp at 500 mW/cm², ~1.5×10¹⁸ photons/cm² s).

ln σ_0 vs E_σ, and identify two different regimes: The data can be fitted by two exponentials demonstrating the usual Meyer–Neldel behavior[23] as well as the so-called anti-Meyer–Neldel behavior (inversion of the slope):[13,15,24]

$$\sigma_0=\sigma_{00} \exp(E_\sigma/E_0). \quad (4)$$

For E_σ>0.2 eV (compensation regime) we are in the usual Meyer–Neldel behavior (positive slope) with a statistical shift of E_F due to doping.[23] The transport in this regime across the internal potential barriers is believed to be dominated by thermionic emission. Contrary to this, for E_σ<0.2 eV, we conclude that the transport is dominated by tunneling from band states of the Si crystallites through the band-tail states of the intervening amorphous phase. In addition, the plot of σ_{RT} (room temperature dark conductivity) vs E_σ can again be fitted with two exponentials showing, thereby, the consistency of the Meyer–Neldel rule.[13]

During light-soaking experiments the conductivity under illumination σ_{ill} of three different samples was simultaneously monitored (Fig. 6): The intensity of the sodium lamp used (about 500 mW/cm², ~1.5×10¹⁸ photons/cm² s) was controlled by a photodiode in parallel. The behavior of the three samples is rather surprising. While the value σ_{ill} of the undoped material slowly decreases with long-term illumination, in contrast to this, in the compensated sample (0.9 vppm) σ_{ill} seems even to increase slightly with time. The undercompensated probe (0.4 vppm, slightly (n) type) shows a small fluctuation but remains more or less constant over the observed time period. From the plot it seems that all curves are probably converging after long-time illumination to the same point. Analyzing the net photocurrent,

$$\sigma_{photo}=\sigma_{ill}-\sigma_d, \quad (5)$$

before and after degradation we observe that the photocurrents for all three films are hardly affected by long-time light

exposure; furthermore, they have similar values around 3×10^{-4} $(\Omega\,\mathrm{cm})^{-1}$. Thus the variations of σ_{ill} in Fig. 6 are mainly due to changes in the dark conductivity. In fact, the observed decrease of the dark current is accompanied by an increase in the activation energy, meaning that E_F is pushed during degradation towards midgap. Thus light-soaking has less effect (or even practically no effect) on compensated material; a low degradation rate was also found, at least for the **beginning** of degradation, in a previous study done with microdoped a-Si:H films.[25] It is generally said about microcrystalline material that it degrades less than a-Si:H because of a self-limiting mechanism in the formation of the light-induced defects.[2,26] It was further shown in Ref. 2 that the dangling-bond (DB) defect density is proportional to the crystallite size δ, inhibiting thus for films with large crystallites ($\delta>120$ Å) the creation of new detectable DBs through light soaking. As a conclusion, we can say that the degradation rate of μc-Si:H films depends mainly on the density of the already existing defects and on the position of E_F as prevailing in the initial state.

IV. CONCLUSIONS

The VHFGD process favors the deposition of microcrystalline silicon with a high crystalline volume fraction, yielding thereby highly conductive doped μc-Si:H layers, as previously shown;[5] the VHF process is also favorable for the deposition of undoped μc-Si:H films; these can be used as a photovoltaic active material, even though undoped films have basically low activation energies (due to extrinsic impurities and contamination dopants). With low-level boron doping, "compensated" films can be deposited, with the Fermi-level position at midgap.

Compensation of the initial (n)-type material could be achieved here by the introduction of a microdoping technique. The very sharp compensation point obtained corresponds to maxima for the dark conductivity activation energy and the photoconductive gain (photo/dark current ratio) and to a minimum for the dark conductivity.

Light-soaking experiments with a high intensity pressure sodium lamp have shown clearly better stability for the new compensated μc-Si:H than for undoped films. In fact, from our series of films, the compensated one appears to be the most appropriate for solar cell applications—as a new promising stable photoactive material—since it degrades the least, its dark conductivity is the lowest, and its photoconductive gain is the highest. The degradation experiments on compensated μc-Si:H are indeed very encouraging: This new photovoltaic material has now to be explored by light soaking of the whole solar cell device, where all possible effects of degradation (field, interface effects) are taken into account.

Using such compensated material for the implementation of entirely μc-Si:H p-i-n solar cells, the extension of the built-in field into the cell could lately be improved (better field uniformity),[5] compared to previously published results.[9] If the better stability of such all μc-Si:H solar cells can be confirmed, microcrystalline silicon could become a new encouraging thin-film base material that could contribute to a solution to the photovoltaic problem provided the efficiency can be increased close to 10%. The most realistic application of our microcrystalline material remains nevertheless the development of stable tandem structures with a standard amorphous p-i-n bottom cell and an entirely μc-SiC:H p-i-n as top cell. The remaining question is now if the VHFGD process is also favorable for the growth of microcrystalline Si carbide films.

ACKNOWLEDGMENTS

The authors are grateful to S. Dubail for substrate preparation. This work was supported by Swiss Federal Research Grant No. EF-REN (90)045 and (93)032.

[1] D. L. Staebler and C. R. Wronski, Appl. Phys. Lett. **31**, 292 (1977).
[2] H. N. Liu and M. D. Xu, Solid State Commun. **58**, 601 (1986).
[3] M. J. Williams, C. Wang, and G. Lucovsky, Proceedings of the International Meeting on the Stability of a-Si:H, Golden, CO, 1991 (unpublished).
[4] F. Wang, H. N. Liu, Y. L. He, A. Schweiger, and R. Schwarz, J. Non-Cryst. Solids **137&138**, 511 (1991).
[5] R. Flückiger, J. Meier, H. Keppner, M. Götz, and A. Shah, 23rd IEEE PVSC, 1993 (unpublished), p. 839.
[6] K. Prasad, Ph.D. thesis, Institute of Microtechnology, University of Neuchâtel, 1991.
[7] K. Prasad, F. Finger, H. Curtins, A. Shah, and J. Baumann, Mater. Res. Soc. Symp. Proc. **164**, 27 (1990).
[8] K. Prasad, U. Kroll, F. Finger, A. Shah, J.-L. Dorier, A. Howling, J. Baumann, and M. Schubert, Mater. Res. Soc. Symp. Proc. **219**, 469 (1991).
[9] R. Flückiger, J. Meier, H. Keppner, U. Kroll, A. Shah, O. Greim, M. Morris, J. Pohl, P. Hapke, and R. Carius, 11th EC PVSEC 1992 (unpublished), p. 617.
[10] A. A. Howling, J.-L. Dorier, Ch. Hollenstein, U. Kroll, and F. Finger, J. Vac. Sci. Technol. A **10**, 1080 (1992).
[11] C. Wang and G. Lucovsky, 21st IEEE PVSC 1990 (unpublished), p. 1614.
[12] P. G. Lecomber, G. Willeke, and W. E. Spear, J. Non-Cryst. Solids **59&60**, 795 (1983).
[13] G. Lucovsky, C. Wang, M. J. Williams, Y. L. Chen, and D. M. Maher, Mater. Res. Soc. Symp. Proc. **283**, 443 (1993).
[14] P. Hapke, F. Finger, R. Carius, H. Wagner, K. Prasad, and R. Flückiger, J. Non-Cryst. Solids **164–166**, 981 (1993).
[15] A. Rubino, M. L. Addonizio, G. Conte, G. Nobile, E. Terzini, and A. Madan, Mater. Res. Soc. Symp. Proc. **297**, 509 (1993).
[16] H. Curtins, N. Wyrsch, and A. Shah, Electron. Lett. **23**, 228 (1987).
[17] R. Tscharner, D. Fischer, H. Keppner, A. Shah, A. Howling, J.-L. Dorier, and Ch. Hollenstein, PVSEC-6, 1992 (unpublished), p. 311.
[18] H. Richter and L. Ley, Appl. Phys. **52**, 7284 (1981).
[19] J. Y. W. Seto, J. Appl. Phys. **46**, 5247 (1975).
[20] F. Finger, R. Carius, P. Hapke, K. Prasad, and R. Flückiger, Mater. Res. Soc. Symp. Proc. **283**, 471 (1993).
[21] P. Pipoz, E. Sauvain, J. Hubin, and A. Shah, Mater. Res. Soc. Symp. Proc. **258**, 777 (1992).
[22] E. Sauvain, A. Mettler, N. Wyrsch, and A. Shah, Solid State Commun. **85**, 219 (1993).
[23] M. Kikuchi, J. Appl. Phys. **64**, 4997 (1988).
[24] C. Manfredotti, F. Fizzotti, G. Amato, L. Boarino, and M. Abbas, Mater. Res. Soc. Symp. Proc. **283**, 507 (1993).
[25] E. Sauvain, P. Pipoz, A. Shah, and J. Hubin, J. Appl. Phys. **75**, 1722 (1994).
[26] M. Stutzmann, W. B. Jackson, and C. C. Tsai, AIP Conf. Proc. **120**, 213 (1984).